SPACE DIVISION

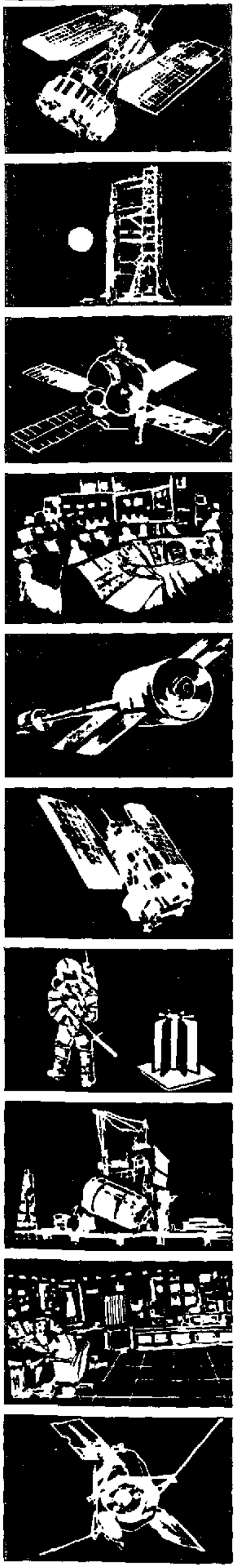

CONTRACT NAS8-29941
22 NOV 1974

NEAR-EARTH THERMAL ENVIRONMENTAL CRITERIA STUDY

(NASA-CR-120592) NEAR-EARTH THERMAL ENVIRONMENTAL CRITERIA STUDY Final Report (General Electric Co.) 41 p HC $3.75 CSCL 20M

N75-16169

Unclas G3/46 08540

FINAL REPORT

GENERAL ELECTRIC

CONTRACT NAS8-29941
22 NOV 1974

NEAR-EARTH THERMAL ENVIRONMENTAL CRITERIA STUDY

FINAL REPORT

PREPARED FOR

GEORGE C. MARSHALL SPACE FLIGHT CENTER
MARSHALL SPACE FLIGHT CENTER, ALABAMA 35812

BY: J.M. DASH
T.F. GREEN
T.P. STARR

SPACE DIVISION
Valley Forge Space Center
P. O. Box 8555 • Philadelphia, Penna 19101

GENERAL ELECTRIC

CONTENTS

LIST OF ILLUSTRATIONS

LIST OF TABLES

1.0 INTRODUCTION

This project is the initial stage of a study to determine improved values and definitions to be used for thermal environmental design parameters for a spacecraft in near-earth orbit. The current criteria is inadequate due to incorrectly assumed confidence limits, the lack of interrelation between albedo and earth thermal radiation, and no altitude dependence. It is planned at a future time to develop the improved criteria through a careful statistical study of known data.

As a starting point, this project was established to convert existing satellite data from selected orbits for which both instantaneous values of the earth thermal and albedo radiation could be obtained, into data which could be easily handled for the planned computer oriented statistic studies.

The Medium Resolution Infrared Radiometer (MRIR) carried onboard the NIMBUS II spacecraft seemed particularly suited to this study since it contained both a 5-30 micron channel to provide a measurement of the earth thermal radiation and a .2-4 micron channel to provide the radiance of the solar reflected radiation (albedo). However, because the lifetime of this instrument was so short it was necessary to use as much of its limited information as possible, to develop a method of utilizing the data from the later NIMBUS III MRIR. The NIMBUS III MRIR sensor had five channels for observing earth radiation.

They were as follows:

6.4 → 6.8 μ		Longwave
10 → 11 μ		
14.5 → 15.5 μ		
20 → 23 μ		
0.2 → 4.0 μ		Albedo

It can be seen, unfortunately, that no single channel covers the entire longwave spectrum as did the Nimbus II MRIR sensor.

Having conducted a thorough literature search in this field, it was found that the NASA Technical Note #D-7249 "The Radiation Balance of the Earth-Atmosphere System from Nimbus 3 Radiation Measurements" by Raschke, Vonder Haar, Pasternak, and Bandeen was most applicable to this project. Goddard Space Flight Center supplied a listing of the program used by Raschke, Vonder Haar et al. to generate their data and the techniques contained within this program were used as a basis for developing the programs used in this project.

A basic concept of the GSFC study was to develop an algorithm whose coefficients could be used to derive a total earth thermal radiation based on a mathematical relationship obtained from studying 160 different atmospheric models. This replaces the need to develop a single algorithm by performing a strictly mathematical correlation of the various spectral bands to the broad band channel of the NIMBUS II data. To produce an output compatible with other studies performed in this field, this same technique was used for this project.

The end product produced by this project is 100 albedo and 100 earth thermal radiation grid maps on 7 track digital magnetic tape. A grid map is a matrix of elements where location in the matrix is related to an earth latitude and longitude. Each value in the matrix is the average of the data over the matrix element area. The size of the matrix element area varies depending on the latitude being observed. The area is 1^o latitude by 1^o longitude at latitudes less than 60^o; 1^o latitude by 2^o longitude at latitudes between 60^o to 80^o, and one area for each polar region at latitudes of 80^o and over. Each map contains the values obtained during a 24 hour period over the entire earth.

No extrapolation was performed on the data, since this will allow greater flexibility for later simulation and Time Average Effective Value (TAEV) computations. The confidence interval widths provided with the statistics for each matrix element area of the earth's surface (data bin) can also be used at some future time for dynamic smoothing of the bin data. It is thought that such autoregressive techniques are superior to any interpolation/extrapolation schemes which could permanently alter the values contained in the constructed data base.

2.0 BRIEF SURVEY OF RESULTS

A brief sample of the output statistics is plotted in the following graphs (Figures 2.0-1 and 2.0-2) to illustrate the type of data generated by the program. The information plotted is the bin averages.

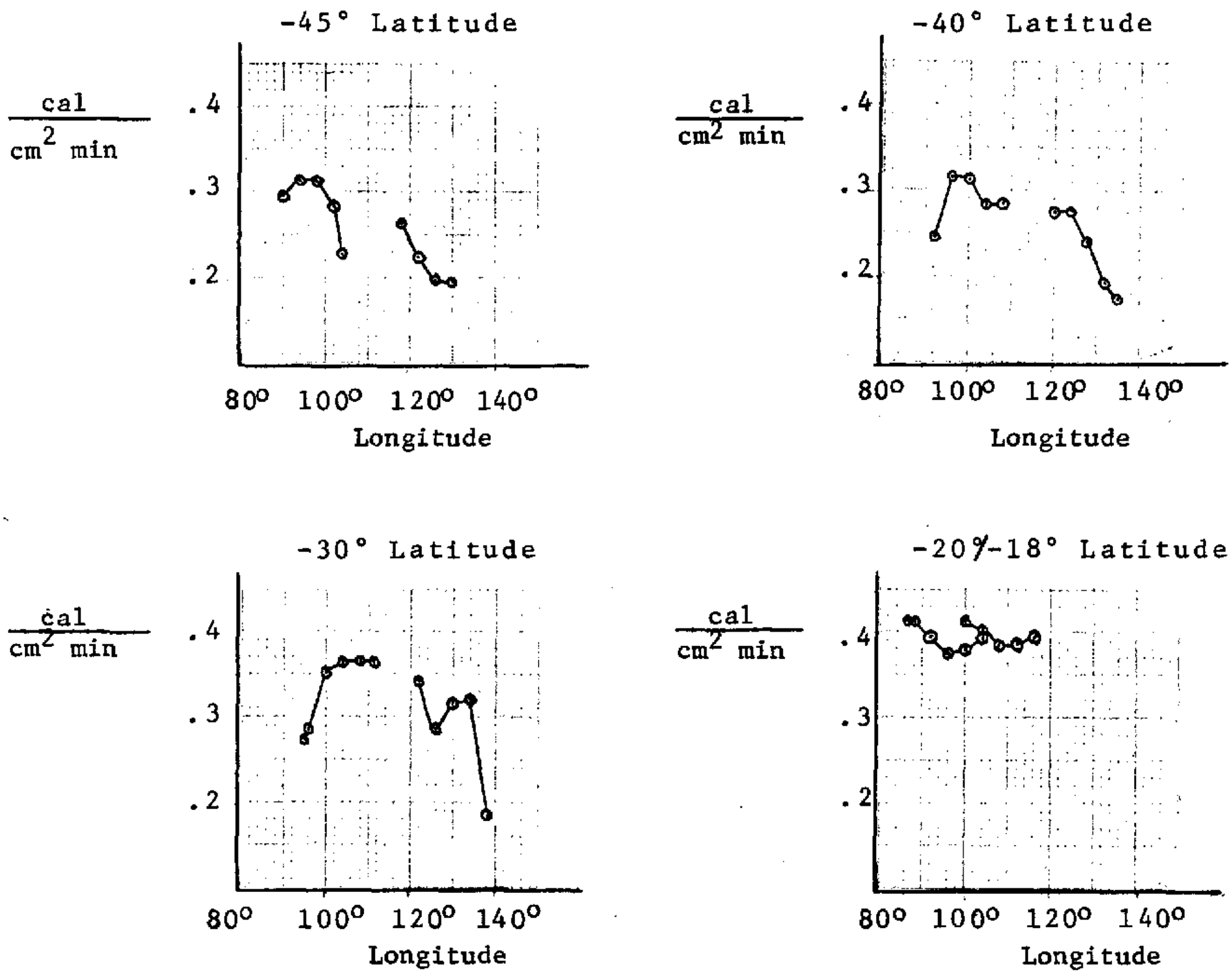

Figure 2.0-1

Outgoing Longwave Radiation (cal/cm^2 min)
Measured by NIMBUS III Day 127, Orbits 315-317

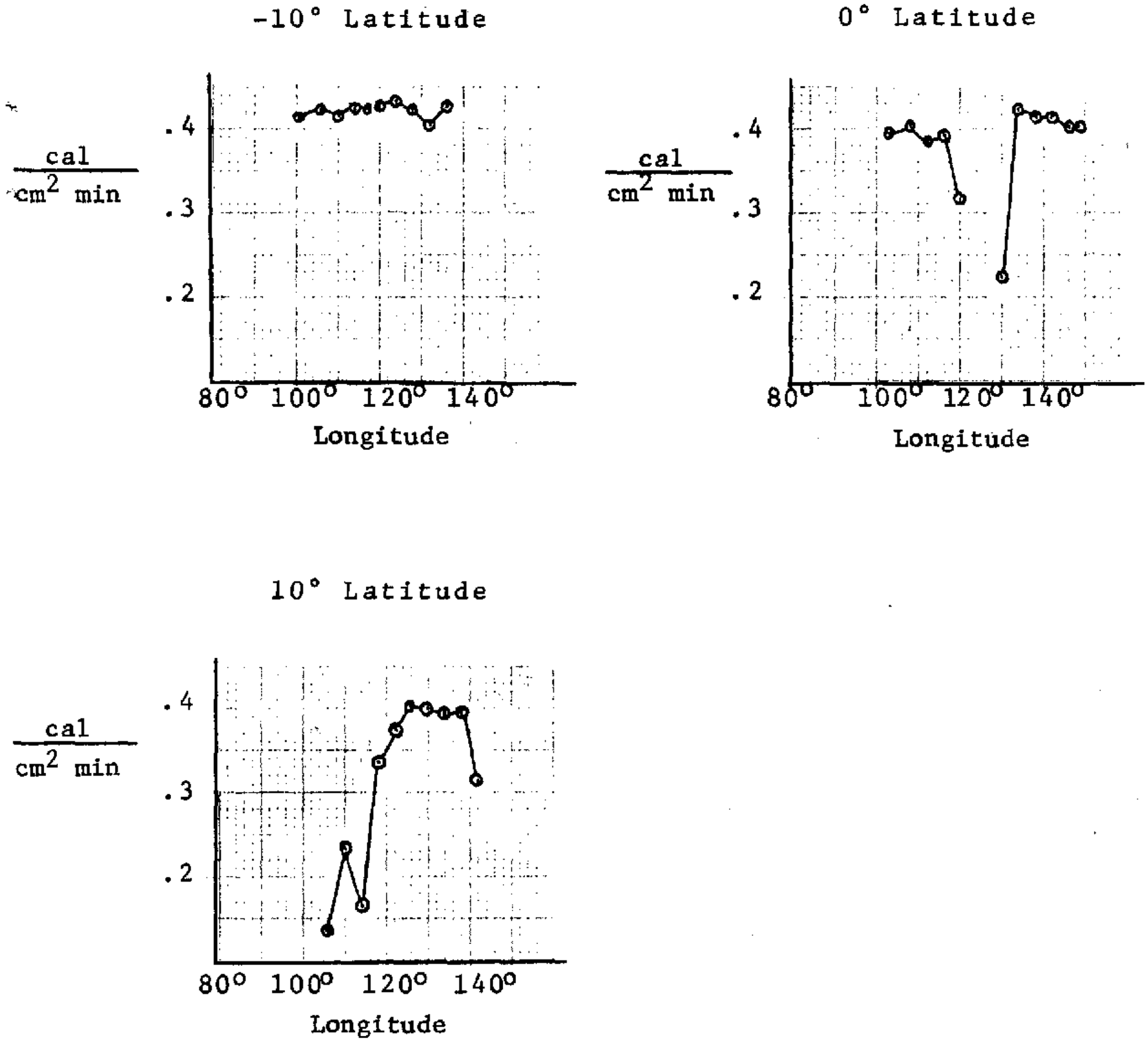

Figure 2.0-1 (cont.)

Outgoing Longwave Radiation (cal/cm^2 min)
Measured by NIMBUS III Day 127, Orbits 315-317

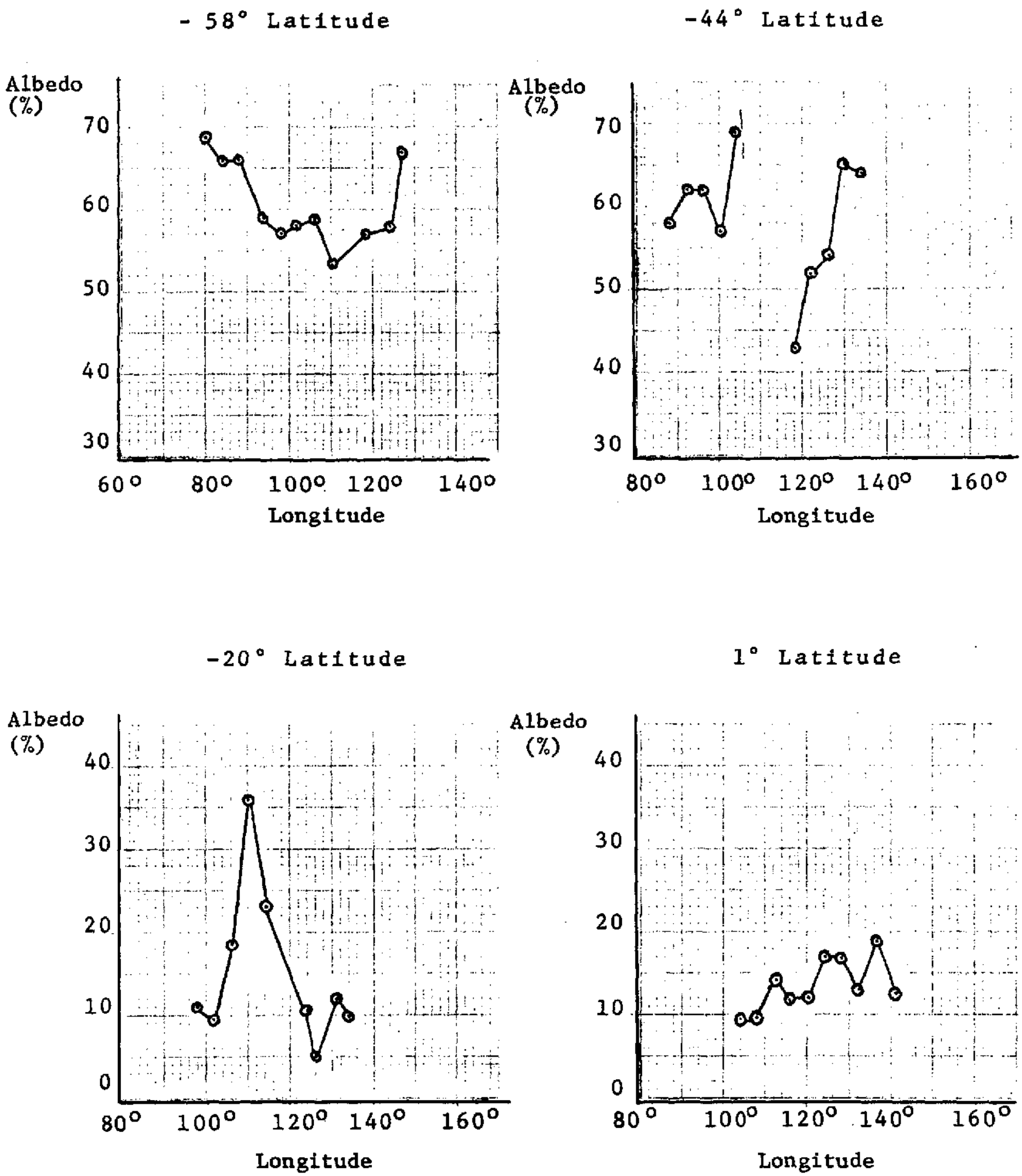

Figure 2.0-2

Albedo (Percent) Daily Averages
Measured by NIMBUS III Day 127, Orbits 315-317

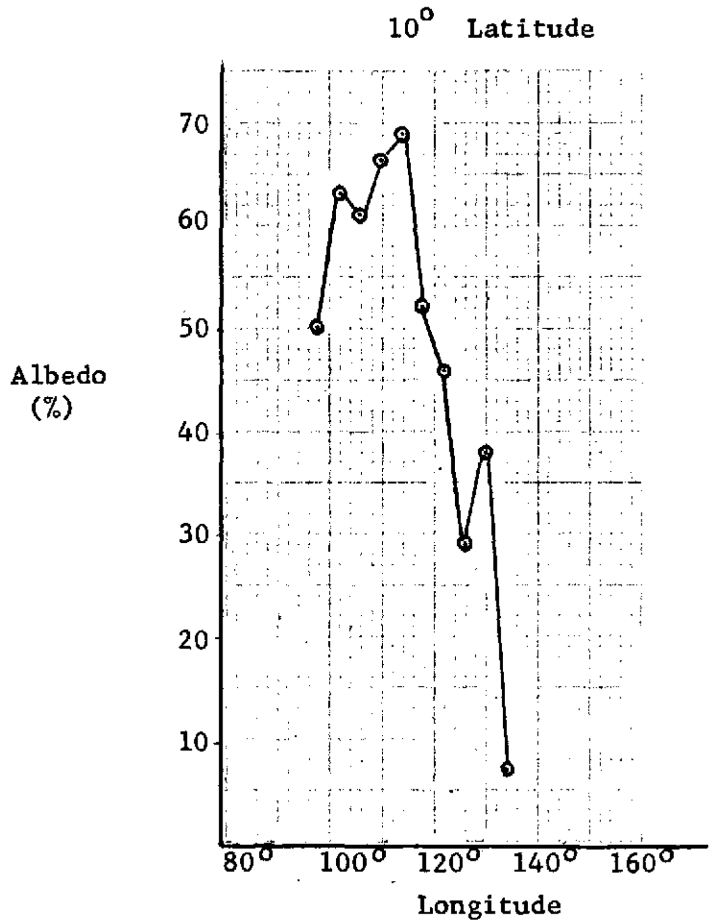

Figure 2.0-2 (cont.)

Albedo (percent) Daily Averages
Measured by NIMBUS III Day 127, Orbits 315-317

A check on the validity of the data produced by the program was made by comparing the data with contour plots of albedo and longwave radiation contained in Appendix D of NASA Technical Note NASA TN D-7249. The values from the contour plots used for the comparison are approximate estimates, however, they do provide indication that the computed values are comparable .

The information is summarized in the following two tables:

Lat.	Long. Range	Computed Range	Data Obtained From NASA TN D-7249
-45	90-130	.19-.32	.30-.33
-40	90-130	.17-.32	.33-.36
-30	90-130	.18-.37	.33-.36
-20/-18	83-118	.37-.42	.39-.42
-10	100-128	.40-.44	.39-.42
0	102-150	.23-.43	.33-.36
10	106-142	.14-.40	.36-.39

Table 2-1
Outgoing Longwave, Nimbus III, Orbits 315-317

Lat.	Long. Range	Computed Range %	Data Obtained From NASA TD D-7249
-58	80-126	44-59	50
-44	28-134	33-60	40
-20	96-134	5-36	20
1	104-142	9-19	20
10	106-142	6-68	20-30

Table 2-2
Albedo (Percent), Nimbus III, Orbits 315-317

3.0 DATA PROCESSING PROGRAM

The program developed for this project, computes estimates of albedo and longwave radiation by extracting the MRIR data from NIMBUS Meteorological Radiation Tapes.

This data is stored by "swaths", each representing a sweep of the rotating scanner. The location of the satellite, time and scan angle associated with the data are sufficient to enable the location of the earth reference area observed by the sensors to be determined.

Following the processing of the data the summary statistics of the radiation estimates are accumulated onto the digital magnetic output tape. These statistics are detailed in Section 5.2 .

A major functional flow of the program is presented in Section 3.1 followed by a detailed description of the steps involved in generating the estimates.

3.1 FUNCTIONAL FLOW DIAGRAM

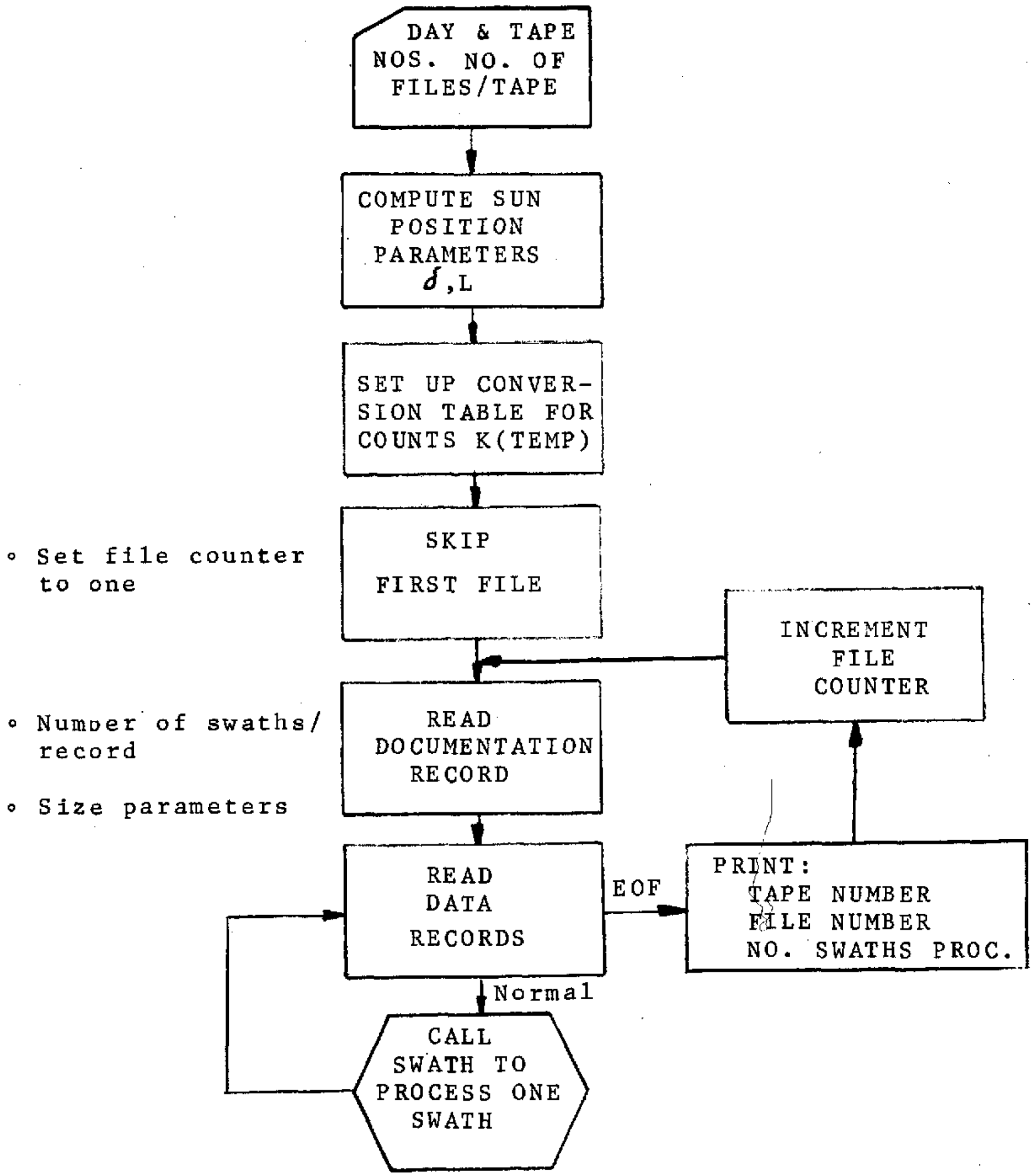

Program SWATH

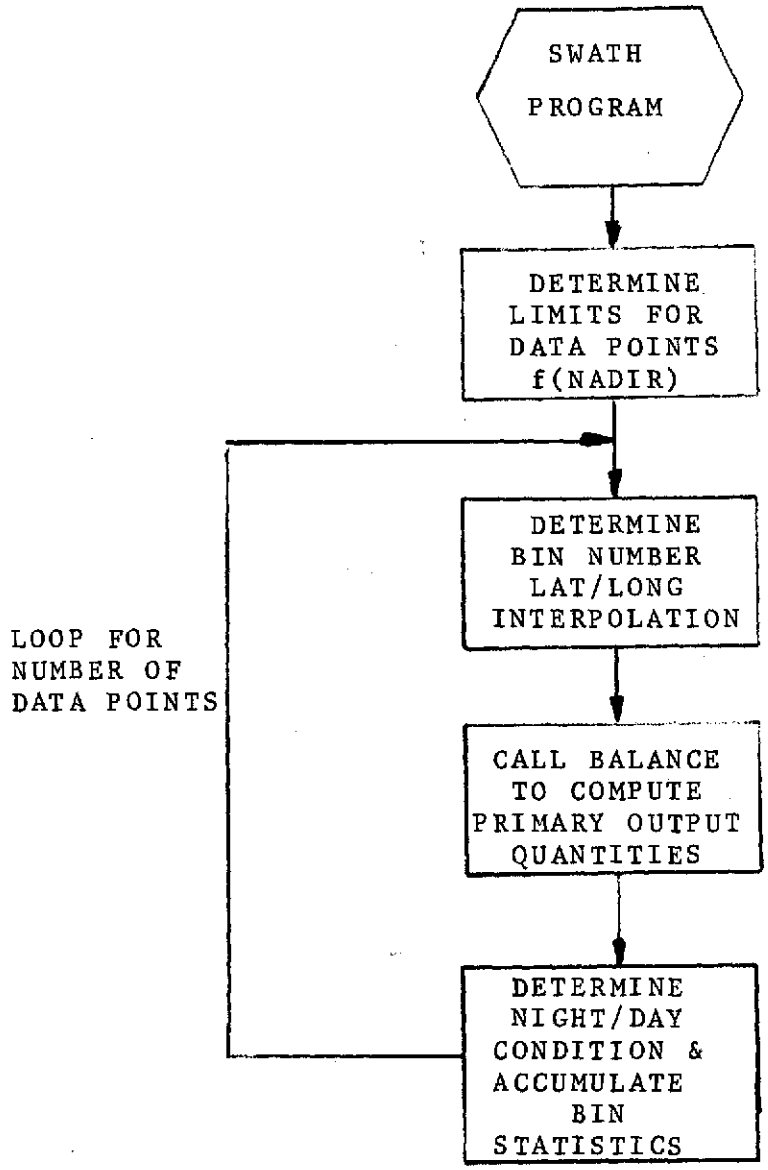

3.1.1 Calculation of the Total Outgoing Longwave Radiation

The two primary processing steps performed by the program in computing the total outgoing longwave radiation are as follows:

Step (a) Estimate the total Longwave Radiation for the entire bandwidth from a NIMBUS II derived correlation formula.

The measured data consists of the filtered radiance observed concurrently by the four channels of the MRIR instrument. Assume that the values from each channel are N_1, N_2, N_3 and N_4 respectively.

$$N_t = \alpha_0 + \alpha_1 N_2 + \alpha_2 N_2^2 + \alpha_3 N_2^3 + \alpha_4 N_4 + \alpha_5 N_1 + \alpha_6 N_3$$

where

$\alpha_0 = -.35651 \times 10^{-2}$

$\alpha_1 = .37442 \times 10^{-2}$

$\alpha_2 = .30818 \times 10^{-3}$

$\alpha_3 = -.92471 \times 10^{-5}$

$\alpha_4 = .013466$

$\alpha_5 = .20913 \times 10^{-2}$

$\alpha_6 = .3051 \times 10^{-2}$

Step (b) Compute the Outgoing Flux Density ($\overline{N}$).

This is obtained by applying a correction which is dependent on satellite location (reference Appendix A for a definition of terms).

The outgoing flux is based on the following estimator:

$$\bar{N}(\lambda,\varphi,t) = 2\pi \int_0^{\pi/2} N_t(\theta,\lambda,\varphi,t)\cos\theta\sin\theta\, d\theta = N_t(\theta=0,\lambda,\varphi,t)\cdot y$$

where $$y = 2\pi \int_0^{\pi/2} f(\theta)\cos\theta\sin\theta\, d\theta \qquad f(\theta) = \frac{N_t(\theta)}{N_t(\theta=0)} \approx \frac{N_{5\text{-}30}(\theta)}{N_{5\text{-}30}(\theta=0)}$$

where $$\frac{N_{5\text{-}30}(\theta)}{N_{5\text{-}30}(\theta=0)} = 1 + \beta_1\theta + \beta_2\theta^2 + \beta_3\theta^3$$

This polynomial model is derived from NIMBUS II data and represents the drop in emitted radiation as θ increases. This radiation model is referred to as "limb-darkening".

It should be noted that the final outgoing longwave flux represents an estimate of the total radiation.

The normal radiation (N_{5-30} (θ =0)) is also derived from NIMBUS II measurements.

Computationally the program uses the following:

For $|\varphi| < 60^\circ$ and;

$$\begin{aligned} \theta < 10^\circ, &\quad \bar{N} = 3.05\ N_t \\ 10^\circ < \theta < 20^\circ, &\quad \bar{N} = 3.054\ N_t/.985 \\ 20^\circ < \theta < 30^\circ, &\quad \bar{N} = 3.054\ N_t/.975 \end{aligned}$$

For $|\varphi| > 60^\circ$ and;

$$\begin{aligned} \theta \le 30^\circ, &\quad \bar{N} = 3.17\ N_t \\ \theta > 30^\circ, &\quad \bar{N} = 3.17\ N_t/.995 \end{aligned}$$

3.1.2 Calculation of the Incoming/Outgoing Solar Radiation (Albedo)

For shortwave or albedo radiation the program computes the average of the outgoing flux densities from the observed data.

The measured data (N') consists of the data from the 0.2-4.0 μ band converted to units of watts/(m^2ster.).* The primary processing steps performed by the program in computing the albedo radiation are as follows:

Step (a) Compute the Bidirectional Reflectance.

The Bidirectional Reflectance is the ratio of the measured data emerging from a surface element in the direction of the satellite to the total radiation entering normal to the surface from space.

$$\rho'(\theta', \psi', \xi'; \lambda, \phi, t) = \frac{N'}{S_o L \cos \xi'}$$

satellite location:
- zenith angle of measurement
- azimuth angle of measurement

solar zenith angle

earth reference longitude

earth reference latitude

time of measurement

$N' = N(\theta', \psi', \xi'; \lambda, \phi, t)$ watts/m^2ster
measured data from the .2-4 μ band

S_o = 860.58 watts/m^2 filtered extra terrestrial radiance of sun (0.2 - 4.0 μ)

$L = \left(\bar{d}/d\right)^2$ $\left\{ \begin{array}{ll} \bar{d} & \text{mean sun-to-earth distance} \\ d & \text{true sun-to-earth distance} \end{array} \right.$

*"Primes" denotes measured data.

Step (b) <u>Compute the approximate directional reflectance.</u>

The directional reflectance can be obtained by using the following theoretical equation:

$$r(\xi) = \int_0^{2\pi}\int_0^{\pi/2} \rho(\theta,\psi,\xi)\sin\theta\cos\theta\, d\theta\, d\psi$$

However, instead of integration, each observed bidirectional reflectance data point can be converted to a directional reflectance point at a specific surface element by using empirical or measured data. The goal being to remove directional (θ,ψ) dependence by use of the ratio

$$\frac{r(\xi=0)}{\pi\rho(\theta',\psi',\xi')}$$

which is available as published tabular data.

The data is stored by:

(1) Surface (cloud-land, ocean, etc.)
(2) ξ
(3) θ
(4) ψ

Definition of item 1 is obtained from the range of ρ' e.g.

(1) Ocean $\pi\rho' < .10$ and $T_b > 273°K$
(T_b being the concurrently observed blackbody temperature)
(2) Snow $|\psi| > 65°$ and $\pi\rho' > .5$
(3) Cloud/land (anything else).

Directional reflectance is computed by

$$r(\xi) = \left[\frac{r(\xi)}{r(\xi=0)}\right]\left[\frac{r(\xi=0)}{\pi\rho(\theta',\psi',\xi')}\right]\pi\rho'$$

Table F-1 Table F-2

It can be seen that r is not a single value, but is a function of two tables; one a function of the surviving independent variable ξ and the other a function of the observed or concomitant angular values (θ', ψ', ξ'). The tables are contained in Appendix F.

Step (c) Estimate the Incoming/Outgoing Radiation

The estimates are derived utilizing the following

$$\text{Incoming }(t) = (S_o L) \cos \xi(t)$$
$$\text{Outgoing }(t) = (S_o L)\, r(\xi) \cos \xi(t)$$

S_o = solar constant
L = reciprocal of sun-earth distance squared in astronomical units

These are integrated over the daylight period for day 't' to arrive at an estimate of the daily averages (see Appendix E).

3.2 THE NIMBUS III DAYS PROCESSED

The following table contains the day numbers for the NIMBUS III data that was processed. An attempt was made to utilize equal daily increments, however this was tempered by determining which days had more representative data and the availability of data tapes.

1969			1970
DAY NUMBER			DAY NO.
107	163	222	21
109	164	223	23
110	166	224	25
112	168	226	28
114	170	228	29
116	172	230	32
118	174	232	34
120	176	234	
122	178	236	
124	180	238	
126	182	239	
128	184	241	
130	186	244	
132	188	246	
134	190	249	
136	192	252	
138	194	256	
140	196	258	
142	198	261	
144	201	264	
147	202	267	
148	204	270	
149	206	273	
151	208	277	
152	210	281	
154	212	285	
156	214	289	
158	216	293	
160	218	298	
161	220	303	

Table 3-1 Day Numbers of Nimbus III Data Processed

4.0 INPUT DATA STRUCTURE

The input data form and content is described in detail in the "NIMBUS III User's Guide" prepared by the NIMBUS Project, Goddard Space Flight Center, National Aeronautics and Space Administration. Section 4 (PP 67-107) deals with the MRIR data which is the principal source of data. The format of the NMRT-MRIR tape is described on PP 99-103 of that document.

5.0 OUTPUT DATA FORMATS

The program produces a digital magnetic tape output containing the daily averages for each bin and selectable line printer output of either summary or detail bin statistics.

The digital magnetic tape is the normal output of the program, the printer output being used during the checkout of the program. However printouts can be requested if desired.

5.1 DIGITAL MAGNETIC TAPE FORMAT

The output tape is a standard 7 track, 800 bpi digital magnetic tape. Each tape may contain more than one data file with each file containing the compiled statistics for one satellite day. The magnetic tape is in Univac 1108 compatible binary format (e.e., formatted 36 bits/word).

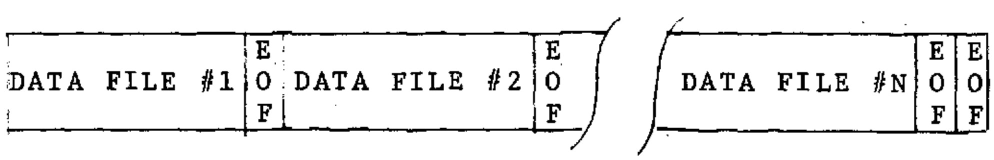

Fig. 5.1-1 Output Tape Gross Format

TYPE 1 RECORD	TYPE 2 RECORD #1	TYPE 2 RECORD #2	.	TYPE 2 RECORD #251	TYPE 2 RECORD #252	TYPE 3 RECORD	EOF

Fig. 5.1-2 Data File Gross Format

As Figure 5.1-2 depicts there are three different types of data records in each file. Every record is equal in size and consists of 1200 words (36 bits per word).

Type 1

The first record of each file is type 1. Word 1 contains the value of the satellite day processed and is the only information contained in this record.

Type 2

Records 2 through 253 of each file are type 2. Each type 2 record contains the statistics for 200 bins, formatted as 6 words for each bin.

The format of each of the 6 word groups is as follows:

<table>
<tr><th>Word no. \ Bit Pos</th><th colspan="2">35 18</th><th colspan="2">17 0</th></tr>
<tr><td>1</td><td colspan="2">Incoming Mean</td><td colspan="2">Outgoing Mean</td></tr>
<tr><td>2</td><td colspan="2">Nighttime Mean</td><td colspan="2">Daytime Mean</td></tr>
<tr><td>3</td><td colspan="2">Outgoing Standard Deviation</td><td colspan="2">Nighttime Standard Deviation</td></tr>
<tr><td>4</td><td colspan="2">Daytime Standard Deviation</td><td colspan="2">Outgoing 95% Confidence</td></tr>
<tr><td>5</td><td colspan="2">Nighttime 95% Confidence</td><td colspan="2">Daytime 95% Confidence</td></tr>
<tr><td>6</td><td>Incoming/Outgoing Population</td><td colspan="2">Nighttime Population</td><td>Daytime Population</td></tr>
<tr><td>Bit Pos</td><td>35 24</td><td colspan="2">23 12</td><td>11 0</td></tr>
</table>

Table 5-1
Summary Statistics Format

NOTE: All the data values contained in words 1 through 5 are scaled by 2^{18}; and the value of incoming and outgoing populations are assumed to be equal.

Type 3

The last or record 254 of each file is a type 3 record which contains statistics for the north and south polar regions. The first 6 words of this record relate to the arctic region; the second 6 words, to the antarctic. The 13th word contains information for both polar regions.

In each case words 1-5 are identical in form to words 1-5 of the type 2 record.

Words 6 and 12 of a type 3 record have the following configuration.

BIT POSITION	
35 ... 18	17 ... 0
OUTGOING POPULATION	NIGHTTIME POPULATION

Word 13 of the type 3 record has the following configuration:

BIT POSITION	
35 ... 18	17 ... 0
NORTH POLE DAYTIME POPULATION	SOUTH POLE DAYTIME POPULATION

Records 2-253 of each file each contain the statistics for 200 bins, for a total of 50400 bins. Record 2 contains bins numbered 1-200, Record 3 contains those numbered 201-400, etc.

To relate bin number to the latitude, longitude of the bin, consider that the earth is divided into 5 areas:

Area 1 - Anarctic - Latitude $< -80^o$. Total 1 bin

Area 2 - Latitude $\geq -80^o$ but $< -60^o$. This region is divided into 1^o latitude by 2^o longitude, regions. Total 3600 bins.

Area 3 - Latitude $\geq -60^o$ but $< +60^o$. This region is divided into 1^o latitude by 1^o longitude regions. Total 43200 bins.

Area 4 - Latitude $> +60^o$ but $\leq 80^o$. This region is divided into 1^o latitude by 2^o longitude regions. Total 3600 bins.

Area 5 - Arctic - Latitude $> 80^o$. Total 1 bin.

Records 2 through 19 contain the data gathered from Area 2.

Records 20 through 235 contain the data gathered from Area 3.

Records 236 through 253 contain the data gathered from Area 4.

Record 254 contains the data gathered from Areas 1 and 5.

For example, the statistics for the bins from Area 2 are formatted on the tape as shown in Table 5-2

RECORD	6 WORD BLOCK #	ACCUMULATOR #	LAT. OF DATA	LONG. OF DATA
2	1	1	-80^o	$0^o \leq$ Long. $< 2^o$
2	2	2	-80^o	$2^o \leq$ Long. $< 4^o$
⋮	⋮	⋮	⋮	⋮
2	200	200	-79^o	$38^o \leq$ Long. $< 40^o$
3	1	201	-79^o	$40^o \leq$ Long. $< 42^o$
3	2	202	-79^o	$42^o \leq$ Long. $< 44^o$
⋮	⋮	⋮	⋮	⋮
3	200	400	-78^o	$78^o \leq$ Long. 80^o
19	1	3401	-60^o	$320^o \leq$ Long. $< 322^o$
19	2	3402	-60^o	$322^o \leq$ Long. $< 324^o$
⋮	⋮	⋮	⋮	⋮
19	200	3600	-61^o	$358^o \leq$ Long. $< 360^o$

Table 5-2 Bin-Record Layout Example

5.2 LINE PRINTER OUTPUT

The following items are contained within the statistical printout from the program. Figure 5.2-1 is a sample printout.

1. Daily average of incoming solar radiation (cal/(cm^2 min))
2. Daily average of reflected solar radiation (cal/ cm^2 min))
3. Nighttime outgoing longwave radiation (cal/(cm^2 min))
4. Daytime outgoing longwave radiation (cal/(cm^2 min))
5. Population count for 1-4
6. Sample standard deviation for (2)
7. Sample standard deviation for (3)
8. Sample standard deviation for (4)
9. 95% confidence band(½ width) for mean of (2)
10. 95% confidence band (½ width) for mean of (3)
11. 95% confidence band (½ width) for mean of (4)

Some defining formulas are:

1. Population count n
2. Mean $\overline{X} = \sum X_{j/n}$
3. Standard deviation $S = \sqrt{\dfrac{(X_j - X)^2}{n-1}}$
4. 100α% confidence bands for theoretical bin mean (μ)

   ½ width $= t\frac{s}{\sqrt{n}}$

where "t" is a $(1 - \frac{\alpha}{2})$ percentile of the t distribution.

NUMBER OF EMPTY BINS = 5269
DAY 154

								95% Confidence Level			Populations			
BIN	MEAN(ICO	OUT	NIGHT	DAY)	SIGMA(OUT	NIGHT	DAY)	CONF(OUT	NIGHT	DAY)	NPTS(ICO	OUT	NIGHT	DAY)
1	0.00000	0.00000	0.16256	0.00000	0.00000	0.00571	0.00000	0.00000	0.00324	0.00000	0	0	12	0
2	0.00000	0.00000	0.16554	0.00000	0.00000	0.00524	0.00000	0.00000	0.00340	0.00000	0	0	10	0
3	0.00000	0.00000	0.16764	0.00000	0.00000	0.00378	0.00000	0.00000	0.00245	0.00000	0	0	10	0
4	0.00000	0.00000	0.17170	0.00000	0.00000	0.00597	0.00000	0.00000	0.00462	0.00000	0	0	8	0
5	0.00000	0.00000	0.17633	0.00000	0.00000	0.00287	0.00000	0.00000	0.00174	0.00000	0	0	11	0
6	0.00000	0.00000	0.18076	0.00000	0.00000	0.00486	0.00000	0.00000	0.00264	0.00000	0	0	11	0
7	0.00000	0.00000	0.18166	0.00000	0.00000	0.00474	0.00000	0.00000	0.00242	0.00000	0	0	14	0
8	0.00000	0.00000	0.18430	0.00000	0.00000	0.00301	0.00000	0.00000	0.00233	0.00000	0	0	8	0
9	0.00000	0.00000	0.18870	0.00000	0.00000	0.00529	0.00000	0.00000	0.00326	0.00000	0	0	11	0
10	0.00000	0.00000	0.19237	0.00000	0.00000	0.00288	0.00000	0.00000	0.00164	0.00000	0	0	12	0
11	0.00000	0.00000	0.19614	0.00000	0.00000	0.00621	0.00000	0.00000	0.00375	0.00000	0	0	11	0
12	0.00000	0.00000	0.19706	0.00000	0.00000	0.00398	0.00000	0.00000	0.00224	0.00000	0	0	12	0
13	0.00000	0.00000	0.19591	0.00000	0.00000	0.00496	0.00000	0.00000	0.00393	0.00000	0	0	8	0
14	0.00000	0.00000	0.19944	0.00000	0.00000	0.00656	0.00000	0.00000	0.00425	0.00000	0	0	10	0
15	0.00000	0.00000	0.19696	0.00000	0.00000	0.00711	0.00000	0.00000	0.00382	0.00000	0	0	13	0
16	0.00000	0.00000	0.20064	0.00000	0.00000	0.00769	0.00000	0.00000	0.00504	0.00000	0	0	8	0
17	0.00000	0.00000	0.19715	0.00000	0.00000	0.00511	0.00000	0.00000	0.00306	0.00000	0	0	11	0
18	0.00000	0.00000	0.19445	0.00000	0.00000	0.00549	0.00000	0.00000	0.00312	0.00000	0	0	12	0
19	0.00000	0.00000	0.18767	0.00000	0.00000	0.00348	0.00000	0.00000	0.00193	0.00000	0	0	13	0
20	0.00000	0.00000	0.18673	0.00000	0.00000	0.00444	0.00000	0.00000	0.00446	0.00000	0	0	6	0
21	0.00000	0.00000	0.19028	0.00000	0.00000	0.00550	0.00000	0.00000	0.00296	0.00000	0	0	13	0
22	0.00000	0.00000	0.18914	0.00000	0.00000	0.00658	0.00000	0.00000	0.00336	0.00000	0	0	14	0
23	0.00000	0.00000	0.18799	0.00000	0.00000	0.00620	0.00000	0.00000	0.00321	0.00000	0	0	14	0
24	0.00000	0.00000	0.17818	0.00000	0.00000	0.00703	0.00000	0.00000	0.00356	0.00000	0	0	14	0
25	0.00000	0.00000	0.18377	0.00000	0.00000	0.00943	0.00000	0.00000	0.00810	0.00000	0	0	7	0
26	0.00000	0.00000	0.17780	0.00000	0.00000	0.00447	0.00000	0.00000	0.00220	0.00000	0	0	14	0
27	0.00000	0.00000	0.17698	0.00000	0.00000	0.00605	0.00000	0.00000	0.00306	0.00000	0	0	14	0
28	0.00000	0.00000	0.17246	0.00000	0.00000	0.00463	0.00000	0.00000	0.00263	0.00000	0	0	12	0
29	0.00000	0.00000	0.17190	0.00000	0.00000	0.00424	0.00000	0.00000	0.00275	0.00000	0	0	10	0
30	0.00000	0.00000	0.17586	0.00000	0.00000	0.00421	0.00000	0.00000	0.00230	0.00000	0	0	12	0
31	0.00000	0.00000	0.18042	0.00000	0.00000	0.00365	0.00000	0.00000	0.00236	0.00000	0	0	10	0
32	0.00000	0.00000	0.18026	0.00000	0.00000	0.00224	0.00000	0.00000	0.00153	0.00000	0	0	9	0
33	0.00000	0.00000	0.18561	0.00000	0.00000	0.00238	0.00000	0.00000	0.00154	0.00000	0	0	10	0
34	0.00000	0.00000	0.18327	0.00000	0.00000	0.00740	0.00000	0.00000	0.00443	0.00000	0	0	11	0
35	0.00000	0.00000	0.19034	0.00000	0.00000	0.00731	0.00000	0.00000	0.00373	0.00000	0	0	14	0
36	0.00000	0.00000	0.19049	0.00000	0.00000	0.00535	0.00000	0.00000	0.00304	0.00000	0	0	12	0
37	0.00000	0.00000	0.18654	0.00000	0.00000	0.00855	0.00000	0.00000	0.00495	0.00000	0	0	12	0
38	0.00000	0.00000	0.18379	0.00000	0.00000	0.00726	0.00000	0.00000	0.00412	0.00000	0	0	12	0
39	0.00000	0.00000	0.18275	0.00000	0.00000	0.01091	0.00000	0.00000	0.00616	0.00000	0	0	12	0
40	0.00000	0.00000	0.17514	0.00000	0.00000	0.01794	0.00000	0.00000	0.00871	0.00000	0	0	15	0
41	0.00000	0.00000	0.16274	0.00000	0.00000	0.02076	0.00000	0.00000	0.01254	0.00000	0	0	11	0
42	0.00000	0.00000	0.15818	0.00000	0.00000	0.02148	0.00000	0.00000	0.01263	0.00000	0	0	11	0
43	0.00000	0.00000	0.16271	0.00000	0.00000	0.02516	0.00000	0.00000	0.01286	0.00000	0	0	14	0
44	0.00000	0.00000	0.16379	0.00000	0.00000	0.02208	0.00000	0.00000	0.01431	0.00000	0	0	10	0
45	0.00000	0.00000	0.16936	0.00000	0.00000	0.02692	0.00000	0.00000	0.01520	0.00000	0	0	12	0
46	0.00000	0.00000	0.17697	0.00000	0.00000	0.02406	0.00000	0.00000	0.01293	0.00000	0	0	13	0
47	0.00000	0.00000	0.17122	0.00000	0.00000	0.02909	0.00000	0.00000	0.01652	0.00000	0	0	12	0
48	0.00000	0.00000	0.17733	0.00000	0.00000	0.02632	0.00000	0.00000	0.01509	0.00000	0	0	11	0
49	0.00000	0.00000	0.17934	0.00000	0.00000	0.02535	0.00000	0.00000	0.01143	0.00000	0	0	17	0
50	0.00000	0.00000	0.17790	0.00000	0.00000	0.02800	0.00000	0.00000	0.01509	0.00000	0	0	12	0
51	0.00000	0.00000	0.19167	0.00000	0.00000	0.01700	0.00000	0.00000	0.00865	0.00000	0	0	14	0
52	0.00000	0.00000	0.18296	0.00000	0.00000	0.02616	0.00000	0.00000	0.01513	0.00000	0	0	13	0
53	0.00000	0.00000	0.19789	0.00000	0.00000	0.01554	0.00000	0.00000	0.00883	0.00000	0	0	12	0
54	0.00000	0.00000	0.19066	0.00000	0.00000	0.02634	0.00000	0.00000	0.01163	0.00000	0	0	17	0
55	0.00000	0.00000	0.19705	0.00000	0.00000	0.02277	0.00000	0.00000	0.01224	0.00000	0	0	13	0
56	0.00000	0.00000	0.19882	0.00000	0.00000	0.02185	0.00000	0.00000	0.01063	0.00000	0	0	15	0
57	0.00000	0.00000	0.20692	0.00000	0.00000	0.00991	0.00000	0.00000	0.00563	0.00000	0	0	12	0
58	0.00000	0.00000	0.20818	0.00000	0.00000	0.01134	0.00000	0.00000	0.00570	0.00000	0	0	14	0

Figure 5.2-1

"Detailed" Bin Statistics - Sample Printout

ORIGINAL PAGE IS OF POOR QUALITY

Appendix A

SATELLITE-EARTH-SUN GEOMETRY

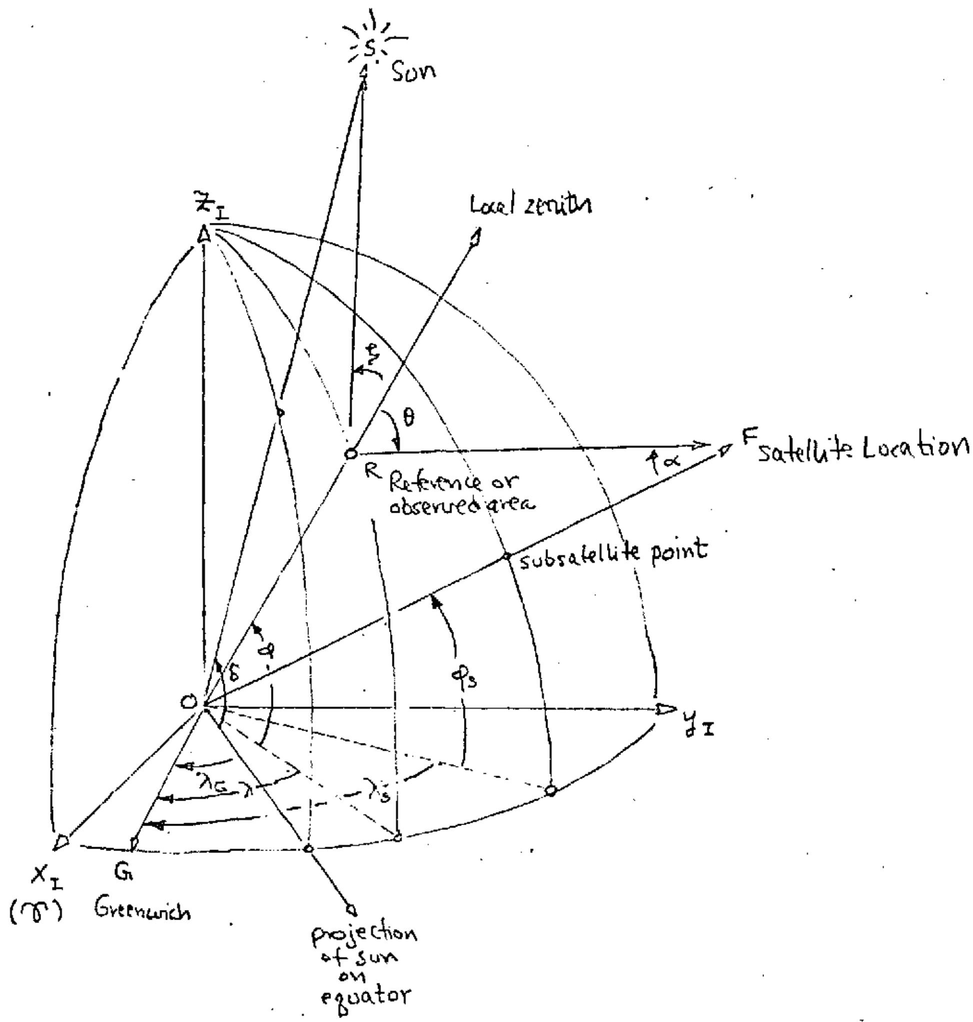

Sun	λ_G	Greenwich hour angle of sun (measured westward)
	δ	Declination of sun
Satellite	λ_S	Longitude of subsatellite point
	φ_S	Latitude of subsatellite point
Observed area	λ	Longitude of observed (reference) area
	φ	Latitude of observed (reference) area

R earth mean radius (6371km)

H satellite altitude (1120km)

Appendix B

LOCAL SUN-EARTH GEOMETRY

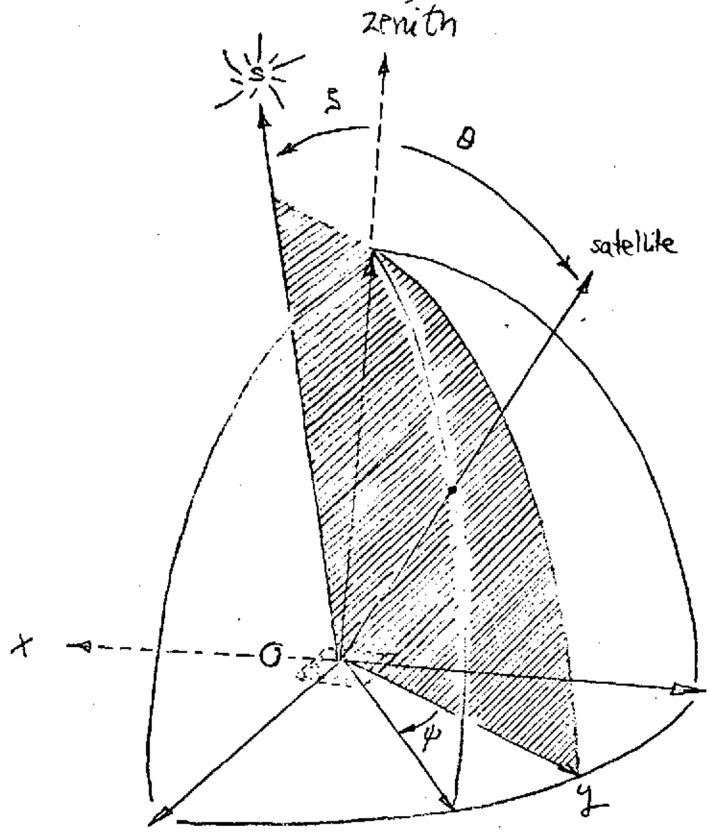

"shaded" region represents the element-sun and element-zenith plane

O - observed area element (bin) centered at (λ, φ).

λ - longitude of observed area

φ - latitude of observed area

ψ - azimuth angle of measurement

- angle between two planes zenith-satellite and zenith-sun measured from the observed area.

θ - zenith angle of measurement

- angle between local zenith and satellite measured from the observed area.

ζ - solar zenith angle

- angle between local zenith and sun measured from the observed area.

The actual observed data is $N(\theta,\psi,\xi)$, which is the radiance emerging from a surface element in the direction of a satellite located at a polar angle θ and azimuth ψ with respect to the sun-vertical plane (see figure). The sun is located at a polar angle ξ with respect to the local vertical.

The total radiation emanating from the surface element can be expressed as:

$$W = \iint N\,dx\,dy$$

From the diagram ψ is measured from y.

To convert to the familiar polar coordinates

$$X = \sin\theta \cos\left(\tfrac{\pi}{2}-(-\psi)\right) = -\sin\theta \sin\psi$$

$$y = \sin\theta \sin\left(\tfrac{\pi}{2}-(-\psi)\right) = \sin\theta \cos\psi$$

$$dxdy = -J\left(\frac{x,y}{\theta,\psi}\right)\, d\theta\, d\psi$$

$$J\left(\frac{x,y}{\theta,\psi}\right) = \begin{vmatrix} \frac{\partial x}{\partial \theta} & \frac{\partial x}{\partial \psi} \\ \frac{\partial y}{\partial \theta} & \frac{\partial y}{\partial \psi} \end{vmatrix} = \begin{vmatrix} -\cos\theta \sin\psi & -\sin\theta \cos\psi \\ \cos\theta \cos\psi & -\sin\theta \sin\psi \end{vmatrix} = \sin\theta \cos\theta$$

Therefore, the total emerging radiation is

$$W = \int_0^{2\pi}\int_0^{\pi/2} N(\theta,\psi) \sin\theta \cos\theta \, d\theta \, d\psi$$

The bidirectional reflectance, a unitless quantity less than one, is the ratio of N to the total energy entering normal to the surface from space

$$\rho(\theta,\psi,\xi) = \frac{N}{S_o L \cos\xi}$$

The <u>directional</u> reflectance is obtained by integrating out the directional dependence on spacecraft position

$$r(\xi) = \int_0^{2\pi} \int_0^{\pi/2} \rho(\theta, \psi, \xi) \sin\theta \cos\theta \, d\theta \, d\psi$$

so that only the sun polar angle remains.

If the surface is considered to be completely diffusing $\rho(\theta, \psi, \xi) = \rho(\xi)$ then:

$$r(\xi) = \int_0^{2\pi} \int_0^{\pi/2} \rho(\xi) \sin\theta \cos\theta \, d\theta \, d\psi = \pi \rho(\xi)$$

Appendix C

MATHEMATICAL RELATIONSHIPS

C - 1 Solar Zenith Angle ξ

$$\cos\xi = \bar{X}\cdot\bar{S} = \cos\delta\cos\phi\cos(\lambda-\lambda_G) + \sin\delta\sin\phi$$

$$\xi = \arccos\left[\cos\delta\cos\phi\cos(\lambda-\lambda_G) + \sin\delta\sin\phi\right]$$

where λ and ϕ are the latitude and longitude of a surface element, λ_G is the Greenwich hour angle and δ is the declination of the sun.

C - 2 Zenith Angle of Measurement θ

$$\frac{\sin\alpha}{r} = \frac{\sin(\pi-\theta)}{r+h}$$

$$\sin(\pi-\theta) = \sin\pi\cos(-\theta) + \cos\pi\sin(-\theta) = \sin\theta$$

$$\sin\theta = \left(\frac{r+h}{r}\right)\sin\alpha$$

If $\theta \geq 50°$ do not process

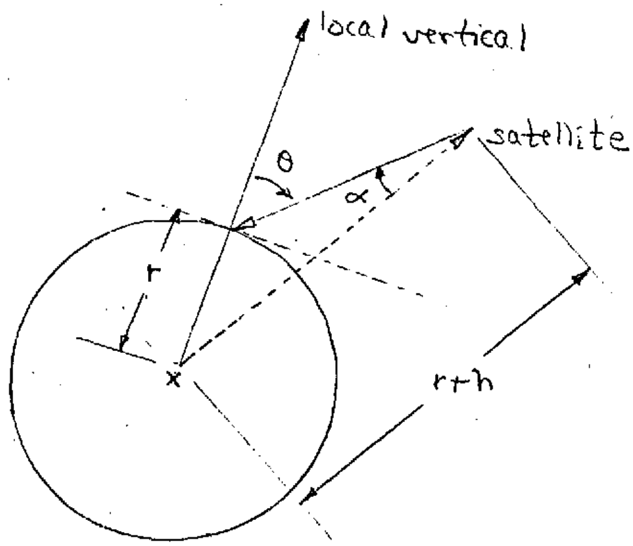

where α is the nadir angle, r the earth's mean radius, and h the satellite height

C - 3 Azimuth Angle of Measurement ψ

$(\bar{S} \times \bar{X})$ perpendicular to sun-zenith plane

$(\bar{X} \times \bar{F}_R)$ perpendicular to zenith-satellite plane

$$\cos\psi = \frac{(\bar{X} \times \bar{F}_R) \cdot (\bar{S} \times \bar{X})}{|\bar{X} \times \bar{F}_R| \, |\bar{S} \times \bar{X}|}$$

simplifying the numerator -

$$\begin{aligned}
(\bar{X} \times \bar{F}) \cdot (\bar{S} \times \bar{X}) &= \bar{X} \cdot (\bar{F}_R \times \bar{S} \times \bar{X}) \\
&= \bar{X} \cdot \left[(\bar{F}_R \cdot \bar{X}) \bar{S} - (\bar{F}_R \cdot \bar{S}) \bar{X} \right] \\
&= \bar{X} \cdot \left[|\bar{F}_R| \cos\theta \, \bar{S} - |\bar{F}_R| \cos\Gamma \, \bar{X} \right] \\
&= |\bar{F}_R| \left[\cos\theta \cos\zeta - \cos\Gamma \right]
\end{aligned}$$

where Γ is the angle between sun and satellite measured at (ϕ, λ).

$$|\bar{X} \times \bar{F}_R| = |\bar{F}_R| \sin\theta$$

$$|\bar{S} \times \bar{X}| = \sin\zeta$$

Therefore

$$\cos\psi = \frac{(\bar{X} \times \bar{F}_R) \cdot (\bar{S} \times \bar{X})}{|\bar{X} \times \bar{F}_R| \, |\bar{S} \times \bar{X}|} = \frac{\cos\theta \cos\zeta - \cos\Gamma}{\sin\theta \sin\zeta}$$

$$\psi = \arccos\left[\frac{\cos\theta \cos\zeta - \cos\Gamma}{\sin\theta \sin\zeta} \right]$$

Define $\kappa = \frac{r+h}{r}$

λ_s longitude of subsatellite point

ϕ_s latitude of subsatellite point

$$\cos \Gamma = \frac{\overline{F_R} \cdot \overline{S}}{|\overline{F_R}|}$$

$$\overline{F_R} \cdot \overline{S} = c\delta\left[k\,c\varphi_s\,c(\lambda_s-\lambda_G) - c\varphi\,c(\lambda-\lambda_G)\right] + s\delta\left[k\,s\varphi_s - s\varphi\right]$$

where "c" and "s" are abbreviated expressions for "cosine" and "sine" respectively.

$$|\overline{F_R}|^2 = \left[k\,c\varphi_s\,c(\lambda_s-\lambda_G) - c\varphi\,c(\lambda-\lambda_G)\right]^2 + \left[k\,c\varphi_s\,s(\lambda_s-\lambda_G) - c\varphi\,s(\lambda-\lambda_G)\right]^2 + \left[k\,s\varphi_s - s\varphi\right]^2$$

$$= k^2c^2\varphi_s\,c^2(\lambda_s-\lambda_G) + c^2\varphi\,c^2(\lambda-\lambda_G) - 2k\,c\varphi_s\,c\varphi\,c(\lambda_s-\lambda_G)\,c(\lambda-\lambda_G)$$
$$+ k^2c^2\varphi_s\,s^2(\lambda_s-\lambda_G) + c^2\varphi\,s^2(\lambda-\lambda_G) - 2k\,c\varphi_s\,c\varphi\,s(\lambda_s-\lambda_G)\,s(\lambda-\lambda_G)$$
$$+ k^2s^2\varphi_s + s^2\varphi - 2k\,s\varphi_s\,s\varphi$$

$$= k^2c^2\varphi_s + c^2\varphi - 2k\,c\varphi_s\,c\varphi\left[c(\lambda_s-\lambda_G)\,c(\lambda-\lambda_G) + s(\lambda_s-\lambda_G)\,s(\lambda-\lambda_G)\right]$$
$$+ k^2s^2\varphi_s + s^2\varphi - 2k\,s\varphi_s\,s\varphi$$

$$= k^2 + 1 - 2k\left[c\varphi_s\,c\varphi\,c(\lambda_s-\lambda_G-\lambda+\lambda_G) + s\varphi_s\,s\varphi\right]$$
$$= k^2 + 1 - 2k\left[c\varphi_s\,c\varphi\,c(\lambda-\lambda_s) + s\varphi_s\,s\varphi\right]$$

$$|\overline{F_R}| = \sqrt{k^2 + 1 - 2k\left[\cos\varphi_s\cos\varphi\cos(\lambda-\lambda_s) + \sin\varphi_s\sin\varphi\right]}$$

Appendix D

SUN ANGLE CORRECTION

The sun angle is corrected for refraction of solar radiation at various angles. This correction reduces the mathematically computed solar zenith angle. The table D-1 contains the corrections used by the program:

$$\xi_{corrected} = \xi_{uncorrected} - \Delta$$

Range	Correction$^{\circ}$ (Δ)
$88^{\circ}.5 < \xi$	.35
$87^{\circ}.5 < \xi < 88^{\circ}.5$	.3
$86^{\circ}.5 < \xi < 87^{\circ}.5$	.235
$85^{\circ}.5 < \xi < 86^{\circ}.5$	.20
$83^{\circ}.5 < \xi < 85^{\circ}.5$	.15
$80^{\circ}.0 < \xi < 83^{\circ}.5$	.10
$\xi < 80^{\circ}.0$	0

Table D-1 Sun Angle Corrections

Appendix E

NUMERICAL INTEGRATION TECHNIQUES

The daily or 24 average of incoming solar radiation over a specific area (λ,φ) is

$$H_s(\lambda,\varphi,t) = \frac{1}{12}\int_{\text{sunrise}}^{\text{sunset}} S_o L \cos \zeta(t^*)\, dt^*$$

where the quantities S_o, L, ζ have been defined earlier.

The flux density of solar radiation leaving the earth-atmosphere system over a specific area (λ,φ) is

$$W_s(\lambda,\varphi,t) = \frac{1}{12}\int_{\text{sunrise}}^{\text{sunset}} S_o L\, r(\zeta) \cos \zeta(t^*)\, dt^*$$

where in both cases, t represents the day of the observation.

Looking first at the 24 hour average of the incoming solar radiation. The theoretical expression is $H_s(\lambda,\varphi,t)$ as described above.

where $S_o = 1.95$ cal $/(\text{cm}^2\text{-min})$
$L = (\bar{d}/d)^2$ reciprocal of squared distance between sun-earth in astronomical units

The numerical approximation used in the program is

$$\hat{H}_s(\lambda,\varphi,t) = \sum_{j=1}^{20} S_o L \cos \zeta[(\lambda-\lambda_\odot)_j]\ \Delta(\lambda-\lambda_\odot)/180$$

= expected incoming radiation.

where $(\lambda-\lambda_\odot)_j$ is the angle between the reference area longitude and the sun projection on the equator.

The quantity is incremented in 20 equal angular increments from sunset to sunrise.

Similarly

$$\hat{W}_s(\lambda,\varphi,t) = \sum_{j=1}^{20} S_o L \cos\xi\left[(\lambda-\lambda_\odot)_j\right] r(\xi)\,\Delta(\lambda-\lambda_\odot)/180$$

The quantity $r(\xi)$ is an extrapolation (from NIMBUS II data) of the observed quantity throughout "all" ξ angles.

Appendix F

TABLES USED IN CALCULATION OF OUTGOING SOLAR RADIATION

The two basic tables used in the albedo computations are presented with three independent variable breakpoints. Table F-1 is used to determine a value for the term $\left\{\frac{r(\zeta)}{r(\zeta=0)}\right\}$ depending on the value of cos ζ. Table F-2 is used to determine a value for the term $\left\{\frac{r(\zeta=0)}{\pi\rho(\theta',\psi',\zeta')}\right\}$ depending on the values of cos ψ , sin θ and cos ζ respectively.

cos ζ	$r(\zeta)/r(\zeta=0)$	
	Ocean	Land
1.00	1.0	1.0
0.954	1.0	1.0
0.901	1.0	1.0
0.848	1.0	1.0
0.795	1.0	1.05
0.742	1.03	1.1
0.689	1.1	1.14
0.636	1.2	1.18
0.583	1.3	1.22
0.530	1.4	1.28
0.477	1.6	1.32
0.424	1.8	1.38
0.371	2.0	1.42
0.318	2.2	1.48
0.265	2.5	1.52
0.212	2.8	1.55
0.159	3.1	1.58
0.106	3.4	1.6
0.053	3.7	1.6
0.0	4.0	1.6

Table F-1

$r(\zeta)/r(\zeta=0)$ Tabulations

The independent variable is cos ζ and it is divided into 20 intervals in order of increasing ζ . Tables F-1 and F-2 are derived from data contained in the RADBAL" computer program developed for Raschke, Vonder Haar, Pasternak and Bandeen.

Table F-2 entries are stored in the order (i, j, k) with the first index moving most rapidly. The breakpoints for i, j, and k are as follows:

i	$\cos\psi$
1	$-1.0 < \cos\psi < -.86603$
2	$-.86603 < \cos\psi < -.5$
3	$-.5 < \cos\psi < 0.$
4	$0. < \cos\psi < .5000$
5	$.5 < \cos\psi < .86603$
6	$.86603 < \cos\psi < 1.$

j	$\sin\theta$
1	$0. < \sin\theta < .17365$
2	$.17365 < \sin\theta < .34202$
3	$.34202 < \sin\theta < .5000$
4	$.5000 < \sin\theta < .64279$
5	$.64279 < \sin\theta < 1$

k	$\cos\xi$
1	$.8195 < \cos\xi < 1$
2	$.5000 < \cos\xi < .8195$
3	$.1736 < \cos\xi < .5000$

$$\left\{ \frac{r(\xi=0)}{\pi\rho(\theta',\psi',\xi')} \right\}$$

OCEAN						LAND					
1.2	1.2	1.3	1.4	1.4	1.4	1.02	1.02	1.02	1.02	1.02	1.02
0.8	1.1	1.3	1.4	1.4	1.4	1.02	1.02	1.02	1.02	1.02	1.02
0.5	0.9	1.25	1.4	1.4	1.4	1.02	1.02	1.02	1.02	1.02	1.02
0.5	0.9	1.25	1.4	1.4	1.4	1.02	1.02	1.02	1.02	1.02	1.02
0.7	1.05	1.25	1.25	1.2	1.2	1.02	1.02	1.02	1.02	1.02	1.02
1.2	1.2	1.2	1.25	1.25	1.3	1.0	1.0	1.0	1.0	1.0	1.0
1.05	1.2	1.2	1.2	1.25	1.35	0.95	0.95	0.95	0.93	0.93	0.93
0.85	1.15	1.2	1.2	1.2	1.35	0.9	0.93	0.93	0.93	0.9	0.9
0.55	0.98	1.15	1.1	1.1	1.25	0.83	0.88	0.93	0.9	0.87	0.87
0.35	0.95	1.15	1.08	1.05	1.1	0.7	0.8	0.85	0.85	0.83	0.83
0.7	0.7	0.7	0.7	0.7	0.7	1.0	1.0	1.0	1.02	1.04	1.04
0.7	0.7	0.7	0.7	0.7	0.7	0.98	0.98	1.0	1.0	1.04	1.07
0.7	0.7	0.7	0.7	0.7	0.7	0.93	0.93	0.97	1.0	1.04	1.04
0.7	0.7	0.7	0.7	0.7	0.7	0.8	0.86	0.93	0.97	0.97	0.97
0.7	0.7	0.7	0.7	0.7	0.7	0.7	0.74	0.86	0.92	0.87	0.84

Table F-2

$r(\xi=0)/\pi\rho(\theta',\psi',\xi')$ Tabulations

NOTE: The table values are shown reading from left to right, and are to be interpreted as shown in the following example.

i	j	k	value for OCEAN
1	1	1	1.2
2	1	1	1.2
3	1	1	1.3
4	1	1	1.4
5	1	1	1.4
6	1	1	1.4
1	2	1	0.8
2	2	1	1.1
3	2	1	1.3
4	2	1	1.4
⋮	⋮	⋮	⋮
6	5	3	0.7